Aminoacetone oxidase from *Streptococcus oligofermentans* belongs to a new three-domain family of bacterial flavoproteins

Gianluca Molla*†[1], Marco Nardini‡, Paolo Motta*, Paola D'Arrigo†§‖, Walter Panzeri‖ and Loredano Pollegioni*†

*Dipartimento di Biotecnologie e Scienze della Vita, Università degli Studi dell'Insubria, via J.H. Dunant 3, 21100 Varese, Italy
†The Protein Factory, Centro Interuniversitario di Biotecnologie Proteiche, Politecnico di Milano, ICRM CNR Milano, and Università degli Studi dell'Insubria, Varese, Italy
‡Dipartimento di Bioscienze, Università degli Studi di Milano, 20133 Milano, Italy
§Dipartimento di Chimica, Materiali ed Ingegneria Chimica G. Natta, Politecnico di Milano, Piazza Leonardo da Vinci 32, 20133 Milano, Italy
‖CNR-Istituto di Chimica del Riconoscimento Molecolare, Politecnico di Milano, via Mancinelli 7, 20131 Milano, Italy

Received 29 July 2014/26 September 2014; accepted 30 September 2014 Published as BJ Immediate Publication 30 September 2014

INTRODUCTION

Streptococci represent ~20 % of bacteria in the human oral cavity, a challenging environment for bacterial survival because it often undergoes rapid and harsh changes in nutrient availability, pH and oxygen concentration. Among the 25 species of oral streptococci, some species can switch from commensal micro-organisms to opportunistic pathogens; i.e. *Streptococcus mutans* is responsible for the development of the two most prevalent oral infectious diseases: dental caries and periodontitis [1]. *Streptococcus oligofermentans* only exists on healthy dental plaques because it is able to outcompete *S. mutans* [2]. Indeed, *S. oligofermentans* employs both lactic acid (one of the main products of *S. mutans* metabolism) and several L-amino acids as nutrients and produces hydrogen peroxide (H_2O_2) [3,4]. Such a capacity was proposed to arise from the product of the aao_{So} gene (GenBank® accession number EU495328) [4], acquired by *S. oligofermentans* through a horizontal gene transfer event [5]; this process may have been important in extending the ecological niche occupied by this *Streptococcus* strain.

The aao_{So} gene encodes a 43 kDa flavoprotein [SoAAO (*S. oligofermentans* aminoacetone oxidase)], which was successfully expressed as a recombinant protein in *Escherichia coli* [4]. This enzyme was reported to possess a low catalytic activity (<0.5 unit/mg of protein) against several different L-amino acids, the best substrates being L-aspartate, L-tryptophan, L-lysine and L-isoleucine. For this reason, it was originally classified as an LAAO (L-amino acid oxidase) (EC 1.1.3.2) [4], despite the absence of any significant sequence similarity with known prokaryotic or eukaryotic LAAOs, except for the sequence motif typical of the dinucleotide binding required for FAD binding [6–8].

LAAO is an FAD-containing enzyme that catalyses the stereoselective oxidative deamination of L-amino acids to yield the corresponding α-keto acids, ammonia and H_2O_2 [9]. This flavoenzyme occurs widely in snake and insect venom [10], but also in several fungi, bacteria (e.g. *Rhodococcus opacus*, *Bacillus carotarum*, *Streptomyces endus* and *Pseudomonus* sp. P-501) and algae (for a comprehensive review, see [9]). On the structural side, LAAOs belong to the N-terminal FAD-bound reductase family and share with DAAO (D-amino acid oxidase) (EC 1.4.3.3) the hydride-transfer mechanism of dehydrogenation [11,12]. LAAOs are promising biocatalysts for a number of biotechnological applications since they catalyse the same reaction as DAAO, but on the opposite enantiomer [9,13]; their biotechnological

Abbreviations: DAAO, D-amino acid oxidase; HRP, horseradish peroxidase; LAAO, L-amino acid oxidase; SoAAO, *Streptococcus oligofermentans* aminoacetone oxidase; SSAO, semicarbazide-sensitive amine oxidase.

[1] To whom correspondence should be addressed (email gianluca.molla@uninsubria.it).

[2] The atomic co-ordinates and structure factors of *Streptococcus oligofermentans* aminoacetone oxidase (SoAAO) have been deposited in the PDB under accession codes 4CNJ and 4CNK, for the native SoAAO and for the complex between SoAAO and *O*-methylglycine respectively.

[3] The nucleotide sequence of the gene coding for *Streptococcus oligofermentans* aminoacetone oxidase has been deposited in the DDBJ, EMBL, GenBank® and GSDB Nucleotide Sequence Databases under accession number KC344836.

application is hampered by difficulties inherent to large-scale production as recombinant proteins [9].

Recently, the *aao*$_{So}$ gene was found as part of an operon together with *mut*T, a gene coding for a specific pyrophosphohydrolase (8-oxo-dGTPase) involved in the elimination of the mutagen-oxidized deoxynucleoside triphosphate 8-oxo-dGTP [14]. Biochemical studies demonstrated that the SoAAO protein is able to oxidize aminoacetone (a pro-oxidant metabolite), with an activity ~25-fold higher than the activity displayed on L-lysine (0.048 compared with 0.002 units/mg of protein respectively), and that the specific activity values with L-amino acids were ~10–50-fold lower than those reported in the original paper [4], thus lending support to the assumption of aminoacetone as the preferred substrate.

In the present study, we have characterized the SoAAO structure–function relationship. Our results show that this flavoprotein fold is based on a specific three-domain architecture, unrelated to that of LAAOs, that SoAAO displays peculiar biochemical properties and does not show LAAO activity. Such results support a specialized role for SoAAO in the microbial defence mechanism related to aminoacetone catabolism through a mechanism yielding dimethylpyrazine derivatives instead of methylglyoxal, as instead proposed for SSAOs (semicarbazide-sensitive amine oxidases) (EC 1.4.3.21) [15].

MATERIALS AND METHODS

Design, synthesis and cloning of cDNA coding for SoAAO

The synthetic cDNA coding for SoAAO was designed by *in silico* back translation of the amino acid sequence reported in GenBank® (accession number ACA52024) [4]. Codon optimization for expression in *E. coli* was performed according to the Codon Usage Database (http://www.kazusa.or.jp/codon/) by eliminating rare codons, i.e. codons used with a $<10\%$ frequency for coding a given amino acid. Synthetic cDNA was produced by GeneArt®. The cDNA molecule coding for SoAAO was cloned into pET24b (Novagen) expression vector between the NdeI and XhoI restriction sites, producing a C-terminal His_6-tagged recombinant protein.

Growth conditions, protein expression and purification

For protein expression, pET24-SoAAO plasmid was transferred into *E. coli* BL21(DE3)pLysS host cells (Novagen) [16,17]. Starter cultures were prepared from a single colony of *E. coli* cells carrying the recombinant plasmid growing at 37 °C on LB broth medium (10 g/l Bacto tryptone, 5 g/l yeast extract and 5 g/l NaCl), to which the antibiotics kanamycin (30 μg/ml final concentration) and chloramphenicol (34 μg/ml final concentration) were added. For protein purification trials, 2 litre baffled flasks containing 500 ml of LB medium were inoculated with the starter culture (initial D_{600} of 0.1) and grown at 37 °C under shaking (220 rev./min) until a D_{600} of 0.8 was reached. Protein expression was induced by adding 1 mM (final concentration) IPTG. To promote the expression of the holoprotein form of recombinant SoAAO, 1.2 μM FAD was also added at the moment of IPTG addition. Cells were harvested by centrifugation at 8000 ***g*** for 10 min at 4 °C 3 h after adding IPTG and were stored at − 20 °C.

Cells were lysed by sonication (six cycles of 30 s each, with 30 s intervals) on ice in 50 mM Tris/HCl (pH 8.0), 40 μM FAD, 0.5 mM PMSF, 1 mM 2-mercaptoethanol and 10 μg/ml DNase I. Cell lysates were centrifuged at 39000 ***g*** for 1 h at 4 °C. The crude extract was loaded on a HiTrap chelating column (GE Healthcare) pre-loaded with Ni^{2+} and equilibrated in 50 mM sodium pyrophosphate (pH 7.2), 1 M NaCl, 20 mM imidazole, 10 μM FAD, 2.5 mM 2-mercaptoethanol and 5 % (v/v) glycerol [17]. The bound protein was eluted from the column using 20 mM sodium pyrophosphate (pH 7.2), 0.5 M imidazole, 10 μM FAD, 1 mM 2-mercaptoethanol and 5 % (v/v) glycerol. The pure protein was then transferred in storage buffer (20 mM Tris/HCl, pH 8.0) by chromatography on a PD10 desalting column (GE Healthcare).

Enzyme activity assay

SoAAO activity on L-amino acids was assayed using a standard continuous spectrophotometric method via determination of H_2O_2 with an enzyme-coupled assay using 1 unit of HRP (horseradish peroxidase) (Sigma–Aldrich) and 0.32 mg/ml *o*-dianisidine, assuming a $\Delta\varepsilon_{440}$ of 13.0 $mM^{-1}\cdot cm^{-1}$ (final volume of 1 ml) [18]. This assay was performed in 50 mM sodium pyrophosphate buffer (pH 7.5–8.5), using 10–100 mM L-amino acid as the substrate at 25 °C.

The activity of SoAAO on aminoacetone was determined at 37 °C using both continuous and discontinuous assays. In the continuous assay, 28 μg of pure SoAAO (0.43 μM final concentration) were mixed with 25 mM aminoacetone (Fluorochem), 1.5 mM 4-aminoantipyrine and 5 units of HRP in 20 mM Tris/HCl (pH 8.0) (assay volume of 1.0 ml). Enzymatic activity was determined from the increase of absorbance at 505 nm: because of the stoichiometry of the reaction, in which two molecules of H_2O_2 react with one molecule of 4-aminoantipyrine, the concentration of produced H_2O_2 (corresponding to the concentration of oxidized aminoacetone) is twice the concentration of quinoneimine produced [18]. The continuous assay was also performed using *o*-dianisidine as the colorimetric reagent; in this case, 130 μg of pure SoAAO, 0.32 mg/ml *o*-dianisidine and 2 units of HRP in 20 mM Tris/HCl (pH 8.0) (assay volume of 0.8 ml) were used; enzymatic activity was determined from the increase of absorbance at 440 nm [18]. In the discontinuous assay, the reaction mixture (1.5 ml) contained 2 μM (133 μg) SoAAO and 12.5 mM aminoacetone or L-aspartate in 20 mM Tris/HCl (pH 8.0). The reaction mixture was incubated at 37 °C for 30 min and then the H_2O_2 produced was quantified using the *o*-dianisidine/HRP-coupled assay. Briefly, 650 μl of the reaction mixture was added to 600 μl of the solution containing 4-aminoantipyrine and phenol (see above): the reaction proceeded for 4 min at room temperature, and then HRP was added (at 0.05–5 units/ml final concentration: the amount of HRP did not affect the absorbance value recorded). After a further 4 min of incubation at room temperature, the absorbance at 505 nm was recorded [4,18].

The products of SoAAO reaction on aminoacetone was also assayed by measuring the amount of ketoacid produced by reaction with 2,4-dinitrophenylhydrazine [15,19]. Briefly, 2.5 mM aminoacetone (an amount chosen so as to not interfere with the reaction of 2,4-dinitrophenylhydrazine with the reaction products) was mixed with 325 μg of SoAAO in 20 mM Tris/HCl (pH 8.0) (2 ml final volume), under stirring at 37 °C: at 0, 15, 30 and 120 min, a 500 μl aliquot was withdrawn and mixed with 150 μl of 10 mM 2,4-dinitrophenylhydrazine, incubated for 10 min at 37 °C and then 1050 μl of 2 M NaOH was added. The visible absorbance spectrum of the mixture was recorded and the ketoacid product was quantified from the absorbance at 518 nm using a molar absorption coefficient of 5.432 $mM^{-1}\cdot cm^{-1}$ estimated from a calibration curve obtained under identical conditions using standard methylglyoxal (Fluorochem).

One unit of SoAAO is defined as that amount of enzyme which produces 1 μmol of H_2O_2 in 1 min at 37 °C.

SDS/PAGE electrophoresis, Western blot and isoelectric focusing analyses

Protein samples from expression trials were analysed by SDS/PAGE; gels were stained for proteins with Coomassie Blue R-250. For Western blot analysis, proteins were transferred on to an Immobilon-P transfer membrane (Millipore) and recombinant SoAAO was identified using anti-His_6-tag mouse monoclonal antibodies (His-probe H-3) and HRP-conjugated goat anti-(mouse IgG) antibodies (all from Santa Cruz Biotechnology). The immunorecognition was detected using the ECL Plus Western Blotting Detection System (GE Healthcare).

Determination of the isoelectric point under non-denaturing conditions was carried out in a flatbed apparatus, FBE-3000 (GE Healthcare), using a 6 % (w/v) polyacrylamide gel slab containing 2.5 % (v/v) of both Pharmalyte 5–8 and Pharmalyte 3–10 (GE Healthcare). As anodic and cathodic solutions 1 M H_3PO_4 and 1 M NaOH were used respectively. The gel was stained for proteins with Coomassie Blue R-250.

Spectral measurements

Absorbance spectra in the UV–visible region were recorded using a Jasco V-560 spectrophotometer. Absorbance data were recorded at 15 °C in 20 mM Tris/HCl, pH 8.0, except where stated otherwise. Anaerobic samples were prepared in anaerobic cuvettes by applying ten cycles of evacuation and then flushing with oxygen-free argon. Photoreduction experiments were carried out at 4 °C using an anaerobic cuvette containing 12.4 μM enzyme, 1 mM EDTA and 0.5 μM 5-deazaflavin [20]. The solution was photoreduced using a 250 W lamp and the progress of the reaction was monitored spectrophotometrically [21].

Fluorescence measurements were performed using a Jasco FP-750 spectrophotometer. All fluorescence measurements were performed at 15 °C and at 0.8 mg/ml protein concentration. See [22,23] for details.

CD spectra were recorded using a Jasco J-815 spectropolarimeter equipped with a software-driven Peltier-based temperature controller producing a temperature gradient of 0.5 °C/min and analysed by means of Jasco software. For measurements above 250 nm, the cell path was 1 cm, whereas for measurements in the 190–250 nm region, the cell path was 0.1 cm. All CD measurements were performed in 20 mM Tris/HCl (pH 8.0) at 15 °C [23].

The redox potentials for the oxidized–reduced SoAAO couple were determined by employing the dye equilibration method described previously [21,24] at 15 °C. The enzyme solution (18 μM final concentration) was mixed in an anaerobic cuvette with 0.2 mM xanthine, 5 μM Benzyl Viologen as mediator and reference dye (i.e. a dye possessing a midpoint redox potential $\pm$30 mV from the potential of SoAAO). The cuvette was made anaerobic (see above), and the visible spectrum of the anaerobic enzyme was recorded. The reaction was initiated by adding 0.18 unit of xanthine oxidase from the side arm and the absorbance spectra were recorded until no increase in the 600 nm peak of the Benzyl Viologen final acceptor was evident. The concentrations of the oxidized and reduced forms of SoAAO were determined from the absorbance values at various wavelengths (after subtracting the dye's contribution) [21]. The concentrations of the oxidized and reduced forms of Benzyl Viologen were determined from the absorbance values at 600 nm where the contribution of SoAAO was negligible. The redox midpoint potential E_m for the system at equilibrium was calculated from the Nernst equation (eqn 1):

$$E_{m,SoAAO} = E_{dye} - (2.3\ RT/nF) \cdot \log([\text{oxidized form}]/[\text{reduced form}]) \quad (1)$$

where R is the gas constant (8.31441 $J \cdot K^{-1} \cdot mol^{-1}$), T is the absolute temperature, F is Faraday's constant (9.6485381×10^4 $C \cdot mol^{-1}$) and n is the number of electrochemical equivalents. All potential values are reported compared with the standard hydrogen electrode [21,25].

Determination of the oligomerization state

The oligomerization state of recombinant SoAAO was determined by gel-permeation chromatography on a Superdex 200 HR column (GE Healthcare) using 20 mM Tris/HCl (pH 8.0), 100 mM NaCl and 2 % glycerol as elution buffer.

Crystallization, structure determination and refinement

SoAAO crystals were obtained by vapour diffusion methods in a hanging-drop set-up, mixing 1 μl of protein (at the concentration of 13.3 mg/ml) and 1 μl of reservoir solution consisting of 2.0 M $(NH_4)_2SO_4$, 0.1 M sodium cacodylate or Mes (pH 6.5), and 0.2 M NaCl. Bright yellow crystals (indicative that the bound FAD was oxidized) with average dimensions of 150 μm$\times$50 μm$\times$50 μm, were grown in $\sim$7–10 days at 4 °C. The crystals were transferred to a cryoprotectant solution consisting of 2.2 M $(NH_4)_2SO_4$, 0.1 M sodium cacodylate or Mes (pH 6.5), 0.2 M NaCl and 25 % glycerol before flash-cooling in liquid nitrogen. The native SoAAO crystals, belonging to the orthorhombic space group $P22_12_1$ (four protein molecules in the asymmetric unit), diffracted at 2.7 Å (1 Å = 0.1 nm) resolution. Diffraction data were collected at the European Synchrotron Radiation Facility beamline ID29, and processed with XDS [26] and SCALA [27].

Vapour diffusion co-crystallization experiments on the protein–ligand complex were performed after overnight incubation of SoAAO (final concentration 12.8 mg/ml) with *O*-methylglycine (final concentration 7 mM) at 4 °C. Crystals of the complex were obtained in a hanging-drop set-up under conditions matching those of the native protein. They belong to the orthorhombic space group $C222_1$ (two protein molecules in the asymmetric unit) and diffracted at 2.0 Å resolution. Diffraction data were collected at the ESRF (European Synchrotron Radiation Facility) beamline ID14-4, and processed with MOSFLM [28] and SCALA [27]. Statistics for each data collection are reported in detail in Table 1.

The SoAAO structure was solved by molecular replacement with Phaser [29], using independently the co-ordinates of the nucleotide-binding domain (residues 1–197 and 337–401) and of the remaining protein (residues 198–336) from flavoprotein HI0933 from *Haemophilus influenzae* (PDB code 2GQF) as search models. The two independent solutions were combined into a unique model and refined as rigid bodies using Refmac [30]. The SoAAO sequence was then model-built into the electron density using Coot [31]. The final model, restrained-refined at 2.7 Å ($R_{work} = 18.8\ \%$, $R_{free} = 23.9\ \%$) with Refmac [30], contains four 391-amino-acid-residue chains (1–391), four FAD molecules, 13 sulfate ions, eight glycerol molecules and 72 water molecules, with good stereochemical parameters.

The structure of the SoAAO–*O*-methylglycine complex was determined by molecular replacement using the program Phaser

Table 1 Data collection and refinement statistics

Outer shell statistics are shown within parentheses. R-merge $= \Sigma_h \Sigma_i |I_{hi} - <I_h>| / \Sigma_h \Sigma_i I_{hi}$.

	SoAAO	SoAAO + *O*-methylglycine
PDB code	4CNJ	4CNK
Data collection		
Synchrotron beamline	ESRF ID29-1	ESRF ID14-4
Temperature (K)	100	100
Space group	$P22_12_1$	$C222_1$
Cell dimensions (Å)		
a	78.95	79.80
b	129.28	231.08
c	224.11	124.93
Resolution (Å)	64.68–2.70 (2.85–2.70)	42.41–2.00 (2.11–2.00)
Observations	231169	305537
Unique reflections	68683	77717
Completeness (%)	98.7 (99.8)	99.5 (99.2)
R-merge (%)	10.4 (53.2)	14.9 (56.1)
$I/\sigma(I)$	10.6 (2.4)	9.0 (4.6)
Multiplicity	3.7 (3.7)	3.9 (4.1)
Refinement		
R-factor/R-free (%)	18.8/23.9	16.9/21.2
Residues in the asymmetric unit	4 × 391 (chains A, B, C and D)	2 × 391 (chains A and B)
FAD molecules	4	2
Water molecules	72	704
O-Methylglycine	–	1 (chain A), 2 (chain B)
Glycerol	8	8
Sulfate ions	13	11
Model quality		
Overall B-factor (Å^2)	60.9 (chain A), 66.4 (chain B), 49.2 (chain C), 59.2 (chain D)	24.6 (chain A), 18.3 (chain B)
RMSD from ideal values		
Bond lengths (Å)	0.008	0.011
Bond angles (°)	1.4	1.5
Ramachandran plot		
Most favoured regions (%)	93.5	95.8
Additional allowed regions (%)	6.5	4.2

[29]. The crystal structure of native SoAAO was used as a monomeric search model. The structure was then refined (rigid body and restrained refinement) using the program Refmac [30]. After a few cycles of refinement, the $2F_o$–F_c electron-density map showed structural details that allowed unambiguous modelling of the bound ligand. The final model, restrained-refined at 2.0 Å ($R_{work} = 16.9\,\%$, $R_{free} = 21.2\,\%$) contains two 391-amino-acid-residue chains (1–391), two FAD molecules, three *O*-methylglycine molecules, 11 sulfate ions, eight glycerol molecules and 704 water molecules, with good stereochemical parameters.

All refinement statistics for both protein models are reported in details in Table 1. The stereochemical quality of the model was assessed using MolProbity [32].

Mass spectra analysis

Mass spectra were recorded on a ESI/MS Bruker Esquire 3000 PLUS (Esi Ion Trap LC/MS$_n$ System), by direct infusion of methanol solution of compounds with an infusion rate of 4 μl/min. Then, 400 μl of a solution containing 3.7 mg of aminoacetone hydrochloride (42.4 mM) in 20 mM Tris/HCl buffer at pH 8.0 was treated with 400 μl of SoAAO in the same buffer (0.37 units/ml, 5.7 mg/ml). The pH was adjusted to 8.0 with NaOH. The reactions were conducted at 37 °C on a thermomixer set to 600 rev./min. At regular intervals, 80 μl aliquots of the reaction mixture were withdrawn, diluted with 240 μl of water and stored in ice until MS analysis. Standard aminoacetone shows a peak at m/z 74.5 (molecular mass of 73 g/mol), whereas its 3,6-dimethyl-2,5-dihydropyrazine cyclic form has peaks at m/z 111 and 221 (molecular mass of 110 g/mol, with the second peak corresponding to the $[2M + H]^+$ form). see Scheme 1 for formulae. Standard methylglyoxal shows a peak at m/z 72. All solvents were of analytical grade.

RESULTS

Properties of recombinant SoAAO

Recombinant SoAAO was purified from the crude extract of *E. coli* cells bearing the pET-SoAAO-His plasmid, grown under optimal conditions (i.e. collecting the cells 5 h after the addition of 1 mM IPTG at a D_{600} of ∼0.8). SDS/PAGE and Western blot analyses showed a band at ∼43 kDa corresponding to recombinant SoAAO at ∼1 h, with the highest productivity at 5 h after IPTG addition (representing ∼10 % of the protein content) (see Supplementary Figures S1A and S1B). Western blot analysis of soluble and insoluble fractions from cell lysate shows that ∼50 % of the recombinant SoAAO was expressed as a soluble protein (Supplementary Figure S1B, right-hand lanes). Changing the IPTG concentration (from 0.1 to 5 mM), or adding 1.2 μM FAD to the culture broth simultaneously to IPTG, as suggested by [4], did not affect the level of recombinant SoAAO production. Similarly, no increase in expression of soluble SoAAO was apparent upon decreasing the growth temperature (15 and 25 °C) after induction of protein expression. Metal-chelating chromatography on a HiTrap chelating column allowed the purification of ∼19 mg of SoAAO/litre of fermentation broth

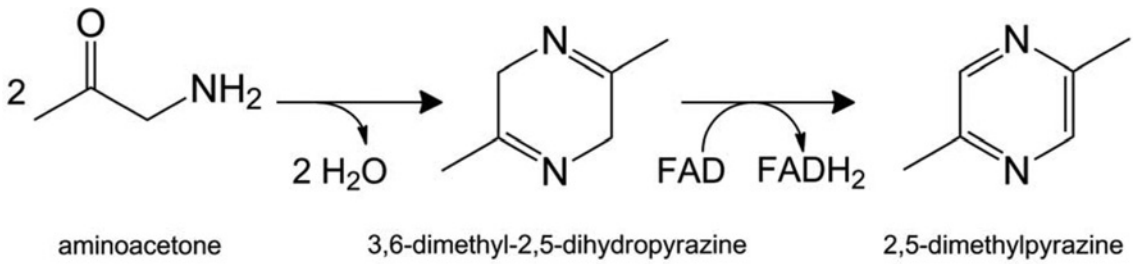

Scheme 1 Proposed reaction catalysed by SoAAO on aminoacetone

The condensation of two molecules of aminoacetone yields 3,6-dimethyl-2,5-dihydropyrazine that is oxidized to 2,5-dimethylpyrazine.

with a purity >90 %, as judged by SDS/PAGE analysis (see Supplementary Figures S1C and S1D). MS analysis yielded a mass for the holoprotein of 43770 Da, in good agreement with the expected value (43744 Da). The isolectric focusing point of the recombinant SoAAO preparation determined under native conditions is 9.1. Gel-permeation chromatography shows that native SoAAO (at a concentration of up to 2.5 mg/ml) eluted as a single peak at ~15.1 ml, corresponding to a molecular mass of ~40 kDa, i.e. as a monomeric enzyme. The oligomerization state of the holoenzyme form of SoAAO differs from that of the snake venom LAAOs, which are stable homodimers in solution [7,9].

Thermal stability of SoAAO was investigated by following changes in the secondary structure, i.e. the CD signal at 208 nm during the thermal ramps. T_m values of 36.9 °C and of 40.4 °C were observed in the absence and in the presence of 10 % glycerol respectively. These results show a relative low thermal stability of SoAAO in comparison with other flavoprotein oxidases from mesophilic micro-organisms such as glycine oxidase from *Bacillus subtilis* (T_m ranging from 56.9 to 63.9 °C), or D-amino acid oxidase from *Rhodotorula gracilis* (T_m of 55.9 °C) [33,34]. Following the decrease in activity of SoAAO at 37 °C (on aminoacetone as substrate, see below), a half-life of ~15 min was estimated.

Notably, no SoAAO enzymatic activity was detected with the crude extract and the purified protein sample on neutral (i.e. L-isoleucine or L-alanine), aromatic (i.e. L-tryptophan or L-tyrosine) L-amino acids as substrates (at 50 mM concentration) using the standard *o*-dianisidine/HRP-coupled assay at 25 °C. Under the same assay conditions, only marginal activity (i.e. overnight colour development) was detected on charged substrates (i.e. L-aspartate or L-lysine).

Spectral properties of recombinant SoAAO

Purified SoAAO in the oxidized form displays the typical absorbance spectrum of FAD-containing flavoproteins, with two absorbance maxima in the visible region at 465 and 370 nm, and a shoulder at ~490 nm (Figure 1A). A molar absorption coefficient of 11990 $M^{-1}\cdot cm^{-1}$ at 465 nm and a ratio of 6.1 between the absorbance values measured at 280 and 460 nm were calculated. The FAD cofactor is not covalently linked to the apoprotein moiety since it is released by heat treatment of the holoenzyme. The absorption spectrum of the cofactor released from the protein (see the broken line in Figure 1A) does not show the 490 nm shoulder, indicating that this spectral feature is not due to FAD chemical modification, but arises from a peculiar hydrophobic environment surrounding the isoalloxazine ring of the cofactor. A similar shoulder is evident when the aromatic ligand benzoate is bound at the active site of D-amino acid oxidase [16]. A soluble apoprotein could not be obtained using various procedures employed previously for several flavoproteins [35,36], e.g. using KBr, urea or guanidine at different concentrations. The fluorescence of the flavin cofactor is only slightly augmented (1.3-fold) in the SoAAO holoenzyme form in comparison with that of free FAD (at pH 8.0).

The far-UV CD spectrum of purified SoAAO shows that the secondary structure of the purified holoprotein is composed of ~35 % α-helices and ~14 % β-sheets (as predicted using the K2D3 server) [37] (see Supplementary Figure S2), in good agreement with the values determined from 3D structure inspection (see Supplementary Figure S3A).

Typically, flavoprotein oxidases stabilize the FAD anionic semiquinone species [38]. Upon SoAAO anaerobic photoreduction, in the presence of 5 mM EDTA and 0.5 μM 5-deaza-FAD, no anionic semiquinone form of the flavin cofactor (in 20 mM Tris/HCl buffer, pH 8.0) could be detected (detection threshold 5 %). After 10 min of light irradiation, the fully reduced flavin species was obtained (Figure 1B); notably, under similar conditions, free FAD is fully reduced by shorter irradiation times, i.e. 6.5 min. When oxygen was admitted to the solution, the oxidized cofactor absorbance spectrum was promptly produced.

The midpoint redox potential of SoAAO was determined at pH 8.0 using the xanthine/xanthine oxidase method and Benzyl Viologen ($E^0 = -359$ mV) as both the mediator and reference dye [24] (Figures 1C and 1D). A midpoint redox potential of -324 mV was estimated, a very low value compared with that for free FAD (-207 mV at pH 7.0) [24] and for typical flavoprotein oxidases, such as yeast D-amino acid oxidase (-130 mV) [21] or glycine oxidase (-298 mV) [22].

The ability to quickly react with sulfite yielding an N(5) covalent adduct (whose spectral properties resemble those of the reduced flavin) distinguishes oxidases from other classes of flavoproteins [12,38]. No spectral changes were observed when SoAAO was added up to 290 mM sodium sulfite; the absorbance spectrum of fully reduced flavin in SoAAO was only obtained when adding simultaneously the reducing agents sodium borohydride and sodium sulfite. Lack of reactivity towards sulfite might result from the absence of a positive (partial) charge in the microenvironment surrounding the flavin N(1)-C(2)=O locus (that inductively promotes the process), or from hampered sulfite diffusion to the cofactor (see below).

SoAAO activity with different substrates

According to [4], the activity of SoAAO was at first assayed on the pure enzyme preparation by measuring the produced H_2O_2 by the standard coupled *o*-dianisidine/HRP method at

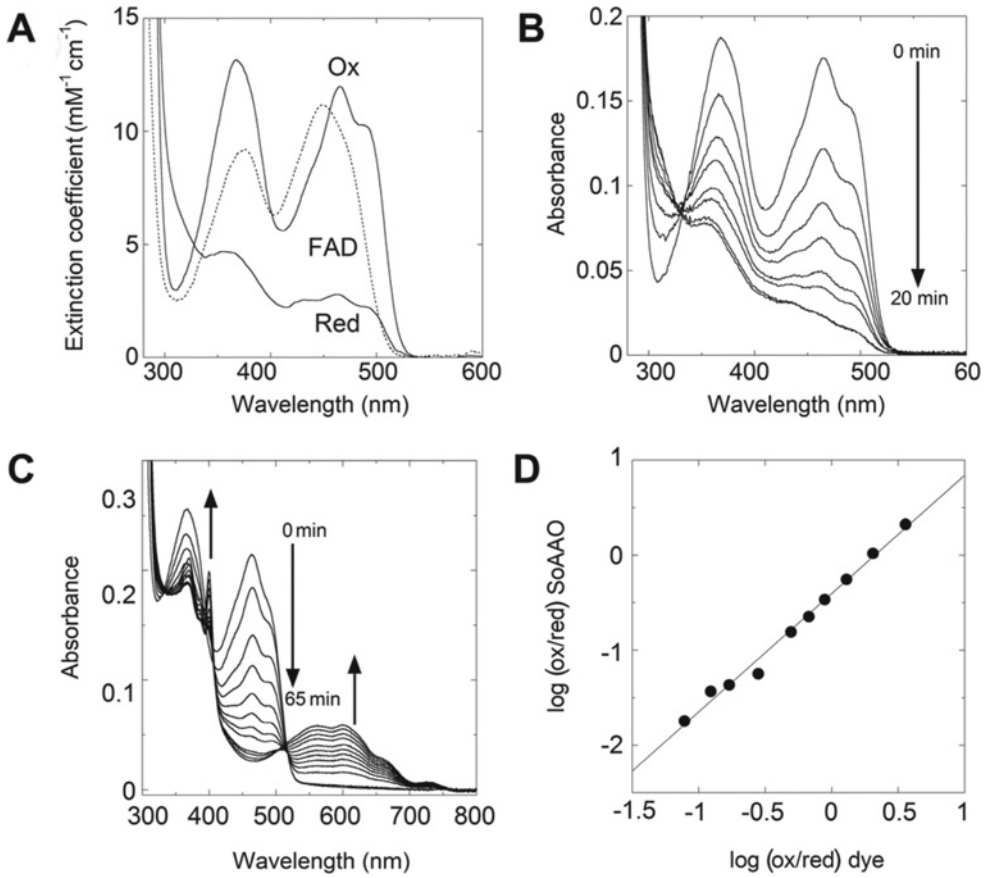

Figure 1 Spectral properties of SoAAO

(**A**) Absorbance spectrum of SoAAO in the oxidized and reduced state at pH 8.0 and 15 °C. The reduced enzyme form was obtained by adding 20 mM sodium borohydride and 20 mM Na_2SO_3. The absorbance spectrum of the FAD cofactor released by SoAAO following heat treatment is represented by the broken line. (**B**) Anaerobic photoreduction of SoAAO in the presence of 5 mM EDTA and 0.5 μM 5-deaza-FAD (4 °C, pH 8.0). The maximal amount of the reduced flavin species was detected after 10 min of photoillumination. (**C**) Determination of the midpoint redox potential (E_m) of SoAAO at pH 8.0. Selected spectra obtained during the course of the anaerobic reduction of SoAAO (18 μM) in 20 mM Tris/HCl (pH 8.0), containing 200 μM xanthine and 5 μM Benzyl Viologen ($E^{0'} = -359$ mV). Spectra were recorded 0, 20, 23, 26, 29, 31, 33, 36, 41, 44, 50, 65 min after the addition of 0.18 unit of xanthine oxidase. (**D**) Nernst plot: the concentration of the oxidized (ox) and reduced (red) forms of SoAAO were determined after subtraction of the dye contribution. The concentration of the oxidized and reduced forms of Benzyl Viologen were determined at 600 nm (where the contribution of the enzyme forms is negligible).

25 °C (see the Materials and methods section and above). In our case, the appearance of a red-brownish colour, evidence of H_2O_2 production, was apparent only after overnight incubation at room temperature in the presence of 10 mM charged substrates (e.g. L-lysine or L-aspartate). This indicates that the O_2-dependent oxidase activity of recombinant SoAAO with L-amino acids is negligible. In contrast, when LAAO from *Calloselasma rhodostoma* was used as a positive control, a specific activity of 3.3 units/mg of protein was measured using L-leucine, in good agreement with the value reported in [39]. Similarly, no conversion of the oxidized form of the flavin cofactor of SoAAO (12.5 μM) into the reduced state was observed following addition of 4.8 mM L-aspartate (or 12.5 mM aminoacetone, see below) under anaerobic conditions at 15 °C.

Recently, it has been proposed that SoAAO could be involved in the oxidation of the small metabolite aminoacetone [14]. To test this hypothesis, we measured the initial rate of H_2O_2 production by mixing 28 μg of SoAAO with 25 mM aminoacetone (at pH 8.0) using the continuous spectrophotometric coupled assay in the presence of 4-aminoantipyrine/HRP [18]. Increasing the temperature of assay to 37 °C, a specific activity with aminoacetone of 0.019 units/mg of protein was measured. The assay was replicated under the same experimental conditions, but using the *o*-dianisidine/HRP method and 130 μg of SoAAO: this yielded a slightly higher specific activity with aminoacetone (0.0298 units/mg of protein) (Figure 2A). A further higher specific activity (0.0463 units/mg of protein) was determined using the most sensitive discontinuous spectrophotometric method: this latter value is very close to the one (0.0478 units/mg of protein) reported in [14]. In comparison, the specific activity with L-aspartate (using the same method) is ~4.5-fold lower (0.013 units/mg of protein). No changes in activity with aminoacetone as substrate was observed upon addition of 1 mM Fe^{2+} or 10 mM Mg^{2+} to the reaction mixture. The very low activity of SoAAO prevented the determination of its kinetic parameters. Indeed, no activity was detected with L-malate, oxaloacetate or α-aminobutyrate (10 mM final concentration).

The SoAAO apparent specific activity value depends on the amount of HRP used as coupling enzyme: 0.016, 0.042 and 0.069 units/mg of SoAAO using 0.04, 0.2 and 2 units/ml HRP respectively (Figure 2B). This effect was obviously not observed when the same coupled method was employed to assay the reaction of a classical oxidase, such as glycine oxidase, since the amount of HRP is broadly higher than the amount required: a specific activity of 0.6–0.7 unit/mg glycine oxidase was determined by using 0.04–2 units/ml HRP. The rate of H_2O_2

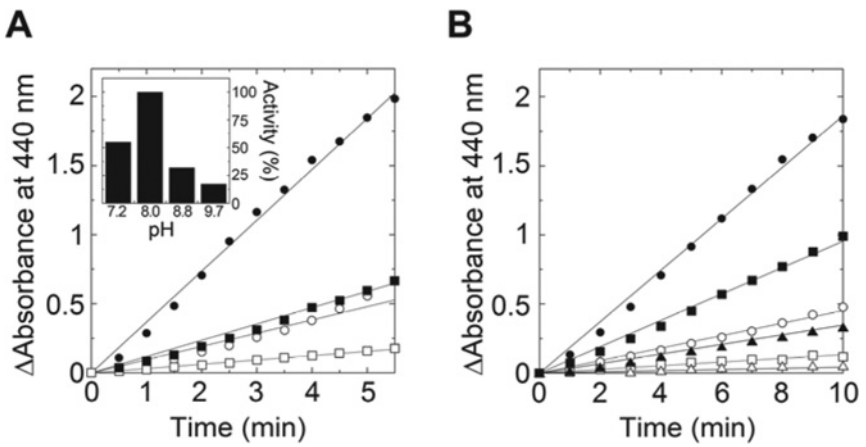

Figure 2 Enzymatic activity of SoAAO on aminoacetone in 20 mM Tris/HCl (pH 8.0) at 37 °C in the presence of 130 μg of SoAAO using 25 mM aminoacetone as substrate (detected using the *o*-dianisidine/HRP method)

(**A**) Initial rate of production of H_2O_2 under vigorous (circles) or moderate (squares) shaking. Inset: pH-dependence of the initial activity (activity measured at pH 8.0 was taken as 100 %). (**B**) Initial rate of production of H_2O_2 in the presence of 2.5 (circles), 0.25 (squares) and 0.05 unit/ml (triangles) HRP with moderate shaking. For both panels, open symbols represents corresponding reactions in the absence of SoAAO (negative controls).

produced starting from 20 mM aminoacetone is ~3.5-fold higher in the presence of SoAAO than in the control assay omitting the flavoprotein (Figure 2B). Notably, aminoacetone is known in aqueous solution to undergo phosphate-catalysed enolysation followed by metal-catalysed oxidation, which is propagated by $O_2^{\bullet -}$ and enoyl aminoacetone radicals, to produce methylglyoxal, H_2O_2 and NH_4^+ ions [40]. In order to avoid such reactivity, all our activity assays were performed in Tris/HCl buffer. Indeed, SoAAO activity was stimulated by vigorous agitation (i.e. higher oxygenation of the reaction mixture) and was higher at pH 8 (Figure 2A, inset).

The effect of SoAAO on aminoacetone was also investigated by analysing the absorption spectrum in alkali of the 2,4-dinitrophenylhydrazone derivative of the reaction products [19]. The absorbance maximum of the mixture after 30 min of reaction does not correspond to that obtained for the standard methylglyoxal (508 compared with ~518 nm; see Supplementary Figure S4). Notably, as expected, the initial activity value determined at 2.5 mM aminoacetone (15 min at 37 °C) is ~0.001–0.003 units/mg SoAAO, a value approximately 10-fold lower than that obtained at 25 mM of the same substrate (0.019 units/mg of protein, see above).

MS analysis of reaction products

SoAAO (0.150 units) was reacted with 21.2 mM aminoacetone in 20 mM Tris/HCl at pH 8.0 and 37 °C and the reaction products were analysed by MS (positive ions). After 1 h of reaction, a new peak at *m*/*z* 109 appeared which corresponds to 2,5-dimethylpyrazine (molecular mass of 108 g/mol, *m*/*z* 109), i.e. the oxidation product of 3,6-dimethyl-2,5-dihydropyrazine (see Supplementary Figures S5A and S5B). After 4 h, the intensity of the peak at *m*/*z* 109 was higher than the peak at *m*/*z* 111 and the peak of free aminoacetone disappeared (see Supplementary Figure S5C). It should be pointed out that the formation of 2,5-dimethylpyrazine also occurs spontaneously, but to a very low extent (as can be observed in the control reaction shown in Supplementary Figures S5D and S5E). Notably, the peak corresponding to methylglyoxal (molecular mass of 72 g/mol, *m*/*z* 73) was never observed, as well as its dimeric and trimeric oligomers. In order to evaluate the effect of H_2O_2 on the reaction products, the enzymatic reaction of SoAAO on aminoacetone has been performed in the presence of catalase (130 units): the intensity of the peak at *m*/*z* 109 observed after 1 h is halved compared with the reaction without catalase (Supplementary Figure S5F).

The 3D structure of SoAAO

The crystal structure of SoAAO has been solved in a binary complex with the oxidized FAD cofactor (2.7 Å resolution, space group $P22_12_1$), and in a ternary complex with FAD and the glycine methyl ester ligand, which mimics the aminoacetone substrate (2.0 Å resolution, space group $C222_1$) (Table 1). In view of the higher resolution achieved, the ternary complex is taken here as a reference for the analysis of the SoAAO structure, unless stated otherwise.

The SoAAO molecule displays an elongated shape, the longer axis being ~85 Å, and the shorter axis being 43 Å. Its tertiary structure is characterized by the presence of three compact domains (Figure 3A). A DALI analysis (http://ekhidna.biocenter.helsinki.fi/dali_server) [41] indicates that domain-1 (residues 1–192 and 328–391) is an α/β domain with FAD/NAD(P)-binding Rossmann-like topology, consisting of a five-stranded parallel β-sheet that is flanked on one side by three α-helices (α1, α2 and α4) and on the other by a three-stranded antiparallel β-sheet and one α-helix (α3) [42]; domain-2 (residues 193–257 and 319–327) has a β-barrel-like topology reminiscent of domain-3 of EF-Tu (elongation factor Tu) [43]; domain-3 (residues 258–318) is mainly α-helical, and similar to the helix–two turn–helix domain of type II DNA topoisomerase VI subunit B [44] (Figure 3A).

The FAD-binding site is located in domain-1. Thirty-nine residues are directly involved in FAD binding (distances below 4.5 Å), of which 11 (Ala^{14}, Glu^{33}, Lys^{34}, Asn^{35}, Ile^{134}, Glu^{362}, Gly^{371}, Gly^{372}, Phe^{373}, Asn^{374} and Ile^{375}) establish electrostatic or polar interactions with the cofactor. Only three of the latter interactions involve side-chain atoms (Glu^{33}, Asn^{35} and Glu^{362}), the others being due to main-chain atoms. Overall, the isoalloxazine ring is quite solvent-exposed, especially at the N5 reactive site, located at the interface between domain-1 and domain-2 (Figure 3B). It establishes hydrogen bonds with the main-chain nitrogen atom of Asn^{374} and of Ile^{375} (FAD O2 atom), and of Gly^{371} (FAD O4

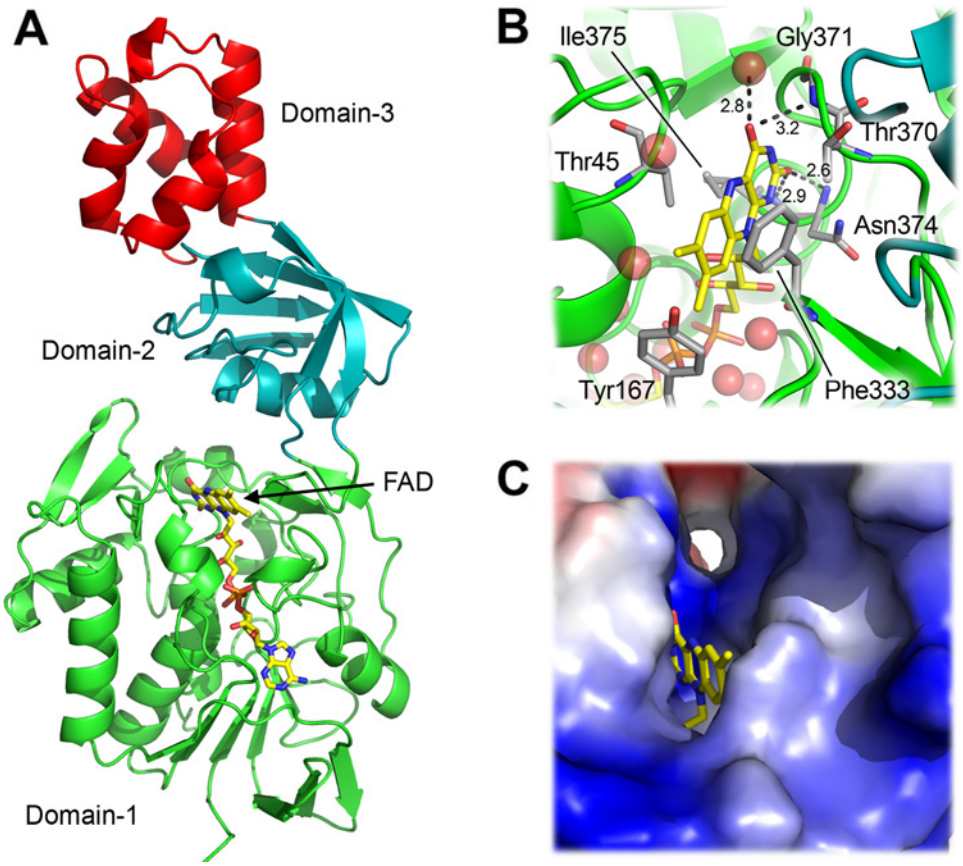

Figure 3 Crystal structure of SoAAO

(**A**) Schematic view of the spatial arrangement of the SoAAO 3-domain fold (domains are displayed in green, cyan and red respectively); α-helices, β-strands and coils are represented by helical ribbons, arrows and ropes respectively. The FAD cofactor bound to SoAAO domain-1 (Rossmann-like topology) is shown in stick representation (yellow colour). (**B**) Protein–FAD interactions and active site cavity of SoAAO. The FAD molecule (yellow) and the protein residues (grey) located at the active-site cavity relevant for FAD binding are shown in stick representation and water molecules are represented as red spheres (0.5 van der Waals radius). Hydrogen bonds are shown by broken lines; numbers represent lengths in Å. The SoAAO active-site cavity is located at the interface between domain-1 (green) and domain-2 (cyan). (**C**) The molecular surface of SoAAO, coloured according to its potential (blue, positive; red, negative). The entry of the active-site cavity, showing the isoalloxazine ring of FAD, is clearly visible. For the sake of clarity, in (**B**) and (**C**), the orientation of the SoAAO structure is slightly different. See also Supplementary Figure S3.

atom), while displaying van der Waals interactions with Thr^{45}, Tyr^{167}, Phe^{333}, Thr^{370} and Ile^{375} side chains (Figure 3C).

Concerning the quaternary structure, the program PISA (http://www.ebi.ac.uk/pdbe/pisa/) [45] did not highlight specific interactions between SoAAO monomers in the crystal that could result in the formation of a stable quaternary assembly, in both the $P22_12_1$ (four protein molecules in the asymmetric unit) and the $C222_1$ crystal forms (two protein molecules in the asymmetric unit); this is in agreement with the results of the gel-permeation experiments on the purified protein (see above).

Overall, the SoAAO tertiary structure resembles that of a putative NAD(FAD)-utilizing dehydrogenase from *Bacillus cereus* (PDB code 2I0Z; DALI *Z*-score of 49.6, residue identity of 46 %), of a flavoprotein from *Sinorhizobium meliloti* (PDB code 3V76; DALI *Z*-score of 47.2, residue identity of 30 %) and of the HI0933 protein from *H. influenzae* (PDB code 2GQF; DALI *Z*-score of 46.5, residue identity of 30 %) (Figures 4A and 4B, and see Supplementary Figure S3B). Unfortunately, all of these proteins structurally related to SoAAO have been analysed within structural genomics initiatives, and neither literature nor functional data are presently available. The structural relationships among the four proteins depend on an excellent conservation of secondary-structure elements in all three domains and on a good match of the FAD-binding site in domain-1 (see Supplementary Table S1). Nevertheless, structural comparison of the protein backbones shows that SoAAO differs markedly from the other three related proteins, both in the orientation of domain-1 relative to domains-2 and -3, and in the precise positioning of the FAD molecule within domain-1 (Figures 4A and 4C). The tertiary structure of SoAAO adopts a more 'closed' conformation, where domain-2 and domain-3 move together as a rigid body (Figure 4B) towards domain-1, thus bringing domain-2 in closer contact to domain-1 relative to 2I0Z, 3V76 and 2GQF tertiary structures (Figure 4A). In SoAAO, few key electrostatic interactions contributed to hook domain-2 to domain-1, specifically Asp^{213} or Asp^{226} to His^{100}, Glu^{194} and His^{369}, and the hydrophobic interaction of the Phe^{333} side chain which fits in a pocket lined by Tyr^{167}, Pro^{196} and Leu^{240}. In 3V76 and 2GQF, site-specific substitutions prevent the formation of such interactions. In the 2I0Z structure, Tyr^{395} is located at the site corresponding to His^{369} in SoAAO, and the salt bridge with Glu^{195} (corresponding to SoAAO Glu^{194}) is therefore not present. Furthermore, despite the sequence conservation, the Phe^{359} side chain (corresponding to SoAAO Phe^{333}) does not fit into the pocket lined by Val^{168}, Pro^{197} and Leu^{250} (corresponding to SoAAO Tyr^{167}, Pro^{196} and Leu^{240}), but moves into the FAD-binding site pocket; the 2I0Z Phe^{359} side

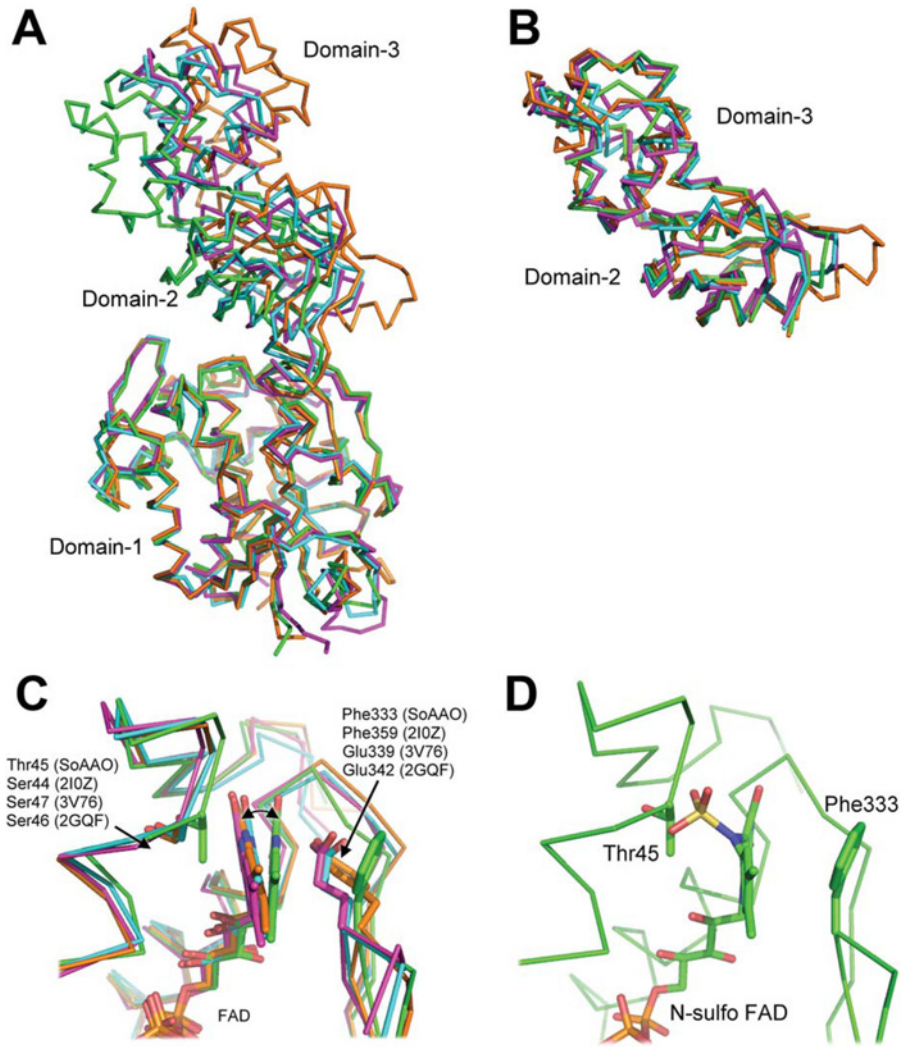

Figure 4 Structural comparison of SoAAO and three structurally related proteins

(**A**) SoAAO (green) is in a more 'closed' conformation, with domain-2 and domain-3 that move as a rigid body towards domain-1 relative to the putative NAD(FAD)-utilizing dehydrogenases from *B. cereus* (PDB code 2I0Z, orange), the flavoprotein from *S. meliloti* (PDB code 3V76, cyan), and the HI0933 protein from *H. influenzae* (PDB code 2GQF, magenta). (**B**) A structural comparison produced by superimposing domain-2 and domain-3 of each protein. The structural superimposition of the isolated domain-2 and domain-3 shows a strong conservation of the tertiary structure and the relative orientation of these domains (see also Supplementary Table S1). (**C**) Orientation of the FAD isoalloxazine ring. Structural superposition of SoAAO FAD-binding site on other structurally related proteins. (**D**) Model of the N5-sulfo-FAD molecule bound to SoAAO based on the isoalloxazine ring of a N5-sulfo-flavin mononucleotide molecule (PDB code 1QCW). Relevant residues are shown in stick representation and labelled.

chain matches the position of 3V76 Glu[339] and 2GQF Glu[342]. As a consequence, the FAD isoalloxazine ring in SoAAO adopts a location that does not match those adopted by the cofactor in the 2I0Z, 3V76 and 2GQF structures, with a maximum shift of ~2.2 Å at the FAD O4 atoms. Such different orientation of the FAD isoalloxazine ring is also related to the substitution of serine for SoAAO Thr[45] in 2I0Z, 3V76 and 2GQF (Figure 4C), and by a backbone shift of the helical region corresponding to SoAAO residues 42–48.

SoAAO in complex with glycine methyl ester

Crystals of SoAAO in complex with aminoacetone could never be grown, probably because of the intrinsic instability and/or enzymatic conversion of aminoacetone under the crystallization conditions. For this reason, we looked for putative SoAAO ligands that could mimic the aminoacetone-binding mode at the active site. The small compound glycine methyl ester (*O*-methylglycine, a molecule significantly more stable in solution than aminoacetone) binds to SoAAO, altering the far-UV CD spectrum (whereas no changes in the UV–visible absorption spectrum were observed). Plotting the changes at 208 nm of the far-UV CD spectra as a function of glycine methyl ester concentration, a K_d of 2.80 $\pm$ 0.46 mM was calculated (see Supplementary Figure S6).

Co-crystallization experiments were performed by incubating SoAAO overnight at 4 °C with a 10-fold molar excess of glycine methyl ester, and resulted in crystals belonging to the $C222_1$ space group (two protein molecules in the asymmetric unit) instead of the native $P22_12_1$ space group (four protein molecules in the asymmetric unit). Despite such crystal packing difference, binding of glycine methyl ester does not alter the SoAAO tertiary structure (RMSD range 0.46–1.03 Å between complex and native structures, depending on the superimposed protein chains), nor promote quaternary assembly of the protein. In both subunits

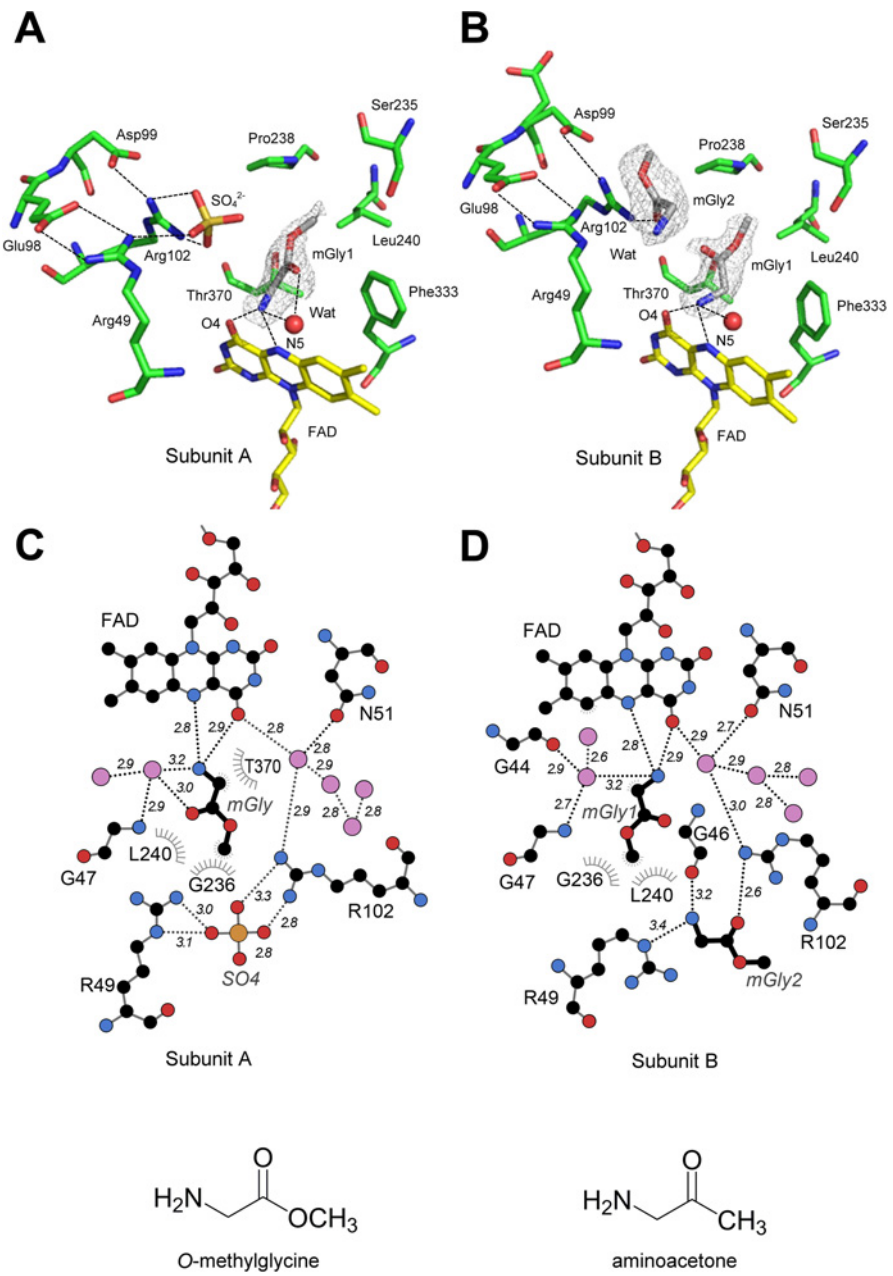

Figure 5 Binding of *O*-methylglycine to SoAAO

(**A** and **C**) Substrate-binding pocket in SoAAO subunit A. (**B** and **D**) Substrate-binding pocket in SoAAO subunit B. The bound *O*-methylglycine (grey: mGly), the FAD molecule (yellow) and the relevant protein residues (green) are shown in stick representation and labelled. Water molecules are shown as red balls. Broken lines indicate hydrogen bonds. The $2F_o–F_c$ electron density (contoured at 1σ) for the bound ligand is shown as a grey mesh. For clarity, Gly[46], whose carbonyl oxygen is hydrogen-bonded to the amino group of mGly2 in subunit B, has been omitted from (**B**) since it overlaps the FAD isoalloxazine ring. For the same reason, some water molecules are not shown. (**E**) Comparison of the chemical structures of *O*-methylglycine and aminoacetone.

of the $C222_1$ crystal form, the glycine methyl ester molecule binds at the interface between domain-1 and domain-2, in a cavity located just on top of the FAD isoalloxazine ring, with the amino group oriented towards the isoalloxazine N5 and the O4 atoms (distances of 2.8 Å and 2.9 Å respectively in both subunits) (Figure 5). The ligand methyl group is hosted in a mostly hydrophobic pocket lined by Ser[235], Pro[237], Leu[240], Phe[333] and Thr[370], whereas the carbonyl oxygen is oriented towards the bulk solvent region in subunit A, and towards the interior of the protein in subunit B (with a rotation along the peptide axis of ~50°). In both subunits, the carbonyl oxygen of the ligand molecule is hydrogen-bonded only with water molecules hosted within the FAD isoalloxazine ring-binding pocket. Interestingly, at the interface between domain-1 and domain-2, the presence of Arg[49] and Arg[102] side chains (kept in position by their salt-bridge interactions with Glu[98] and Asp[99] respectively) generates a positively charged pocket suitable for binding of a sulfate ion, originating from the crystallization solution, in subunit A (Figures 5A and 5C), and for a second *O*-methylglycine molecule in subunit B (Figures 5B and 5D). The presence of a sulfate-trapping pocket at the entrance of the FAD isoalloxazine ring-binding cavity could help to explain the absence of reactivity

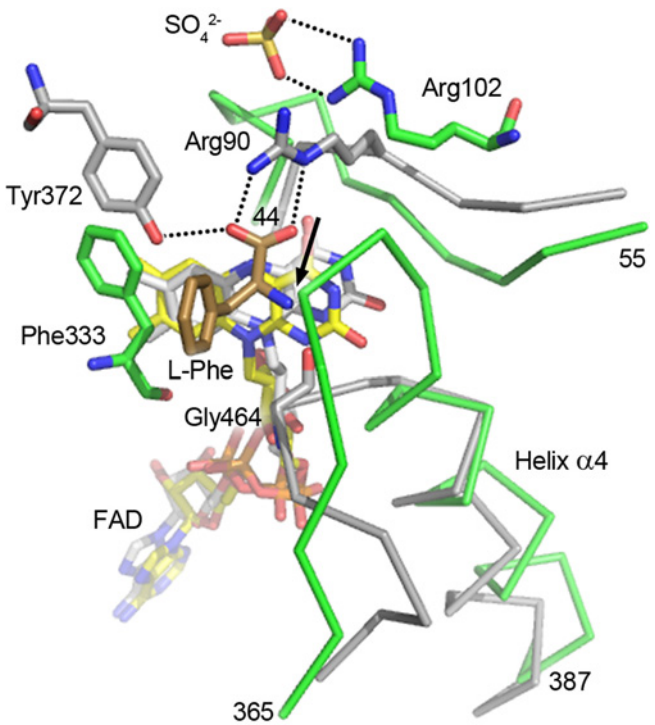

Figure 6 Structural comparison between the SoAAO and LAAO (from *C. rhodostoma*, PDB code 2IID) substrate-binding sites

SoAAO and LAAO residues are shown in green and grey respectively, with SoAAO FAD in yellow, LAAO FAD in grey and LAAO-bound substrate L-phenylalanine in brown. Broken lines indicate relevant hydrogen-bond interactions. For clarity, the Cα backbone of the SoAAO helix α4 and of the 44–57 and 365–387 regions are indicated in ribbon representation, together with the corresponding LAAO regions. The close contact between SoAAO Thr^{370} Cα and the amino group of the L-phenylalanine bound to LAAO is indicated by an arrow.

of SoAAO with sulfite. Furthermore, the model of SoAAO in complex with N5-sulfo-FAD (generated on the basis of the isoalloxazine ring of a N5-sulfo-flavin mononucleotide; PDB code 1QCW), shows that the close vicinity of the SoAAO 3_{10}-helical 42–48 segment to the FAD N5 reactive site would provide steric clash of the bound sulfite with Thr^{45} (Figure 4D), thus preventing sulfite binding. In addition, this unusual feature of a flavo-oxidase is also supported by the absence of positively charged groups in the proximity of the N1-C2=O locus of the isoalloxazine ring, whose presence would inductively promote the process. A partial positive charge may, however, be provided by the dipole associated to the N-terminus of the nearby helix α4. Intriguingly, almost no similarity can be detected between the active-site structural organization and the ligand-binding mode of SoAAO with respect to other known LAAOs [7,9] (Figure 6).

DISCUSSION

In search of biotechnological applications of LAAO activities, we focused on the flavoenzyme produced by *S. oligofermentans*, a member of the 'mitis' group of oral streptococci involved in the initial steps of dental biofilm formation. This FAD-containing enzyme was initially reported to oxidize seven different amino acids, with a specific activity of 0.47 unit/mg of protein (for L-aspartate or L-tryptophan), and to be overexpressed in *E. coli* [4]. The original activity values for L-amino acids reported in [4] were subsequently revised, and aminoacetone was reported as the preferred substrate for purified SoAAO (with a specific activity ~0.048 units/mg of protein) [14]. Genetic analysis based on double deletion of the aao_{So} and *mutT* (encoding a pyrophosphohydrolase which removes mutagens such as 8-oxo-dGTP) genes, and on the observation that inactivation of aao_{So} caused a concentration increase of the pro-oxidant molecule aminoacetone and of the cellular ROS (reactive oxygen species) stress, indicated that SoAAO represents a novel antioxidant defence system in *S. oligofermentans* [14].

In the present study, we designed a synthetic optimized SoAAO-encoding cDNA and expressed the recombinant protein in *E. coli* to up to 19 mg of protein/litre of fermentation broth; previous expression levels were not reported [4,14]. Purified SoAAO is a FAD-containing protein which tightly binds the flavin cofactor: the protein is purified as a holoenzyme, FAD is not released during gel-permeation chromatography, and the apoprotein form could never be produced even using standard procedures previously employed for several flavoenzymes [35,36]. SoAAO does not present the classical properties of the oxidase-dehydrogenase class of flavoproteins [38]. In fact: (i) the FAD cofactor is not reduced by L-amino acids or aminoacetone under anaerobic conditions at 15 °C; the reduced flavin form was only achieved chemically (by adding together sulfite and borohydride-reducing agents) or photochemically (in the latter case, reduced FAD promptly reacted with dioxygen); (ii) it does not produce a semiquinone species when light-irradiated even in the presence of redox mediators (the midpoint redox potential for the two-electron transfer was -324 mV); (iii) it does not react with sulfite to form a flavin N(5)–sulfite adduct, a reaction commonly present in flavo-oxidases [46].

From a structural point of view, SoAAO belongs to a novel protein family. Four bacterial proteins, whose physiological role has not been elucidated, share similar tertiary structure composed of three domains: an α/β domain corresponding to the FAD-binding domain, a β-domain which partially modulates accessibility to the coenzyme, and an additional α-domain. Phylogenetic analysis confirms that SoAAO homologues are present in microorganisms belonging to the genus *Streptococcus* [5] and that they are also widespread in bacteria belonging to the Firmicutes and Proteobacteria phyla with a sequence identity between SoAAO and homologues ranging from 30 % to 45 % (considering the overall sequence). SoAAO homologues were also identified in Viridiplantae (green plants) although with a lower degree of identity with SoAAO (~25 %) (see Supplementary Figure S7).

The *O*-methylglycine molecule bound to SoAAO provides a useful molecular scaffold to mimic the binding mode of aminoacetone, which differs from *O*-methylglycine only in the substitution of the ester group by a methyl ketone (Figure 5E). From a structural standpoint, SoAAO does not resemble known LAAOs, since classic LAAOs are homodimeric holoenzymes (the main exception being those from *E. coli* and *Sulfolobus tokodaii*) [9], whereas SoAAO is monomeric, and LAAO belongs to the N-terminal FAD-bound reductase family while SoAAO is a three-domain protein. LAAOs evolved an active-site arrangement to bind L-amino acids and to discriminate between the two different enantiomers, the so-called four-location model [7]. In all cases, the substrate binds to the LAAO active site on the *re*-face of the isoalloxazine moiety of FAD, with the major interactions being: (i) a salt bridge between the α-COO^- of the amino acid and the guanidinium group of an arginine residue located close to the pyrimidine-derivative ring of the isoalloxazine moiety; this interaction is strengthened by an additional hydrogen bond with the hydroxy group of a tyrosine residue; (ii) a hydrogen bond between the α-amino group of the L-amino acid and the main-chain C=O of the protein belonging to a small residue

(glycine or alanine); (iii) the third anchor point is formed by the region of the active site located above the hydrophobic moiety of the FAD isoalloxazine ring: this latter region accommodates the substrate side chain and represents the main structural determinant of substrate specificities observed in the various LAAOs [9]. In contrast, the overall structure of the SoAAO active site differs markedly from those of LAAOs. In particular, the Cα-backbone of the β5–α4 region (residues 365–373) has a deep impact on the reshaping of the SoAAO ligand-binding site, also affecting the structure of the nearby βA–αB region (residues 44–55) (Figure 6). As a consequence, the tip of the β5–α4 loop partly overlaps with the LAAO substrate-binding site, and the LAAO small residue (glycine or alanine) whose carbonyl oxygen would hydrogen-bond to the α-amino group of the L-amino acid is displaced from the SoAAO substrate-binding site. Furthermore, the arginine residue that in LAAO stabilizes the α-COO^- of the substrate amino acid is not conserved in the SoAAO βA–αB region, being structurally replaced by Arg^{102}, which in SoAAO is involved in shaping the sulfate-trapping pocket (Figure 5). Finally, the tyrosine side chain that in LAAO contributes to stabilize the bound substrate via hydrogen-bonding, is not present in SoAAO, being replaced by Phe^{333}.

The role of the SoAAO domain-2 and domain-3 is unclear. No specific function is associated with the two protein domain modules and, although they form a rigid body conserved among homologous proteins (Figure 4B), their orientation relative to the nucleotide-binding domain (domain-1) may vary depending on the protein considered (Figure 4A). It is interesting to note that in SoAAO, although not promoting dimerization, domain-2 and domain-3 are, however, productively involved in crystal contacts, especially at the interface of the α-helical domain-3 (see Supplementary Figure S8), thus suggesting that the apical domain-3 might represent a structural element involved in recruiting additional partner proteins.

Characterization of the kinetic properties confirmed a very low SoAAO activity with aminoacetone, and a marginal activity with L-amino acids, as reported in a recent report [14], and the production of H_2O_2 when aminoacetone (or L-aspartate) are used as substrates. We demonstrated that SoAAO activity on aminoacetone depended on the amount of HRP used as coupling enzyme (Figure 2A) and that H_2O_2 production is observed also in the absence of the flavoprotein. This observation reconciles the previous specific activity values reported in the literature: the values reported in [4] were determined using 100-fold higher HRP than in [14] (5 and 0.05 units/ml respectively). The amount of HRP seems to play a crucial role in the oxidation of aminoacetone by SoAAO: aminoacetone has been reported to undergo enzymatic (by SSAO) and Fe^{n+}/Cu^{2+}-catalysed oxidation to methylglyoxal, H_2O_2 and ammonia with O_2 consumption [47]. In particular, a haem-containing protein such as ferricytochrome *c* initiated by one-electron transfer, O_2-dependent oxidation of aminoacetone to yield the aldimine of methylglyoxal [NH=CH-C(=O)-CH_3], which then hydrolyses to methylglyoxal [CH_3-C(=O)-C(=O)H], ammonia and H_2O_2 [40]. We propose that a similar role might be played by HRP in the coupled activity assay, thus accounting for the amount of H_2O_2 produced in the absence of SoAAO.

MS and 2,4-dinitrophenylhydrazone-derivative analyses of the reaction products of SoAAO on aminoacetone showed that no methylglyoxal is produced and that the main product is 2,5-dimethylpyrazine. Accordingly, and differently from that proposed for SSAO that converts aminoacetone into methylglyoxal [15], we propose that condensation of two aminoacetone molecules yields 3,6-dimethyl-2,5-dihydropyrazine that is subsequently oxidized to 2,5-dimethylpyrazine (Scheme 1). The ability of SoAAO to bind two molecules of the substrate analogue *O*-methylglycine ligand, as shown in Figure 5(B), is held to facilitate the condensation reaction. Interestingly, the position occupied by Arg^{49} and Arg^{102} in subunit B (Figures 5B and 5D) allows not only the binding of a second molecule of the substrate analogue *O*-methylglycine in the active site of SoAAO, but also proper positioning of the amino group of the second substrate molecule with respect to the carbonyl group of the (first) substrate molecule bound next the isoalloxazine flavin ring. We do not exclude that methylglyoxal and/or H_2O_2 produced by the non-enzymatic spontaneous oxidation of aminoacetone might promote the reaction of SoAAO, since catalase negatively affected the rate of aminoacetone oxidation (see Supplementary Figure S5F).

The low specific activity of SoAAO (the highest value was 47.8 nmol/min per mg of protein) as compared with known amino acid oxidases (up to 120 μmol/min per mg of yeast DAAO, 2 and 60 μmol/min per mg of *E. coli* LAAO and glutamate oxidase respectively) [9,16], poses an open question about the physiological role of this protein. The activity of SoAAO appears to speed up the elimination of aminoacetone in the cell: the aminoacetone levels in *S. oligofermentans* doubled when the *aao* gene was deleted (from 77 pmol/mg per cell for the wild-type strain to 147 pmol/mg per cell for the Δaao_{So} mutant strain), nevertheless reaching a modest concentration [14]. Although SoAAO activity is low, it should be sufficient to control the observed increase in aminoacetone: the very low enzymatic activity of SoAAO with L-amino acids should then just represent a promiscuous activity. Also, we cannot exclude the possibility that SoAAO might play a role as binding protein that senses aminoacetone and, through the recruitment of further binding partners (through the non-catalytic domain-2 and domain-3), would activate/stimulate cell defence mechanisms.

In conclusion, SoAAO represents a member of a novel family of bacterial flavoproteins composed of three domains, unrelated to LAAO activities, and involved in specific functions, such as participating in antioxidant defence from the pro-oxidant metabolite aminoacetone in *S. oligofermentans* by yielding pyrazine derivatives instead of methylglyoxal.

AUTHOR CONTRIBUTION

Marco Nardini grew the crystals and solved the structure of the protein; Gianluca Molla and Paolo Motta performed the biochemical characterization; Paolo D'Arrigo and Walter Panzeri carried out the MS analysis of the reaction products; Loredano Pollegioni and Gianluca Molla conceived the project and wrote the paper. All authors have read and approved the paper.

ACKNOWLEDGEMENTS

We thank Sandro Ghisla and Martino Bolognesi for helpful discussion.

FUNDING

This work was supported by grants from Ministero dell'Istruzione, dell'Università e della Ricerca Scientifica (MIUR) Fondo di Ateneo per la Ricerca to L.P. and G.M. We acknowledge the support from Consorzio Interuniversitario per le Biotecnologie (CIB) and Centro Grandi Attrezzature dell'Università degli Studi dell'Insubria.

REFERENCES

1 Nicolas, G. G. and Lavoie, M. C. (2011) *Streptococcus mutans* and oral streptococci in dental plaque. Can. J. Microbiol. **57**, 1–20 CrossRef PubMed

2 Tong, H. C., Gao, X. J. and Dong, X. Z. (2003) *Streptococcus oligofermentans* sp nov., a novel oral isolate from caries-free humans. Int. J. Syst. Evol. Microbiol. **53**, 1101–1104 CrossRef PubMed

3 Tong, H., Chen, W., Merritt, J., Qi, F., Shi, W. and Dong, X. (2007) *Streptococcus oligofermentans* inhibits *Streptococcus* mutans through conversion of lactic acid into inhibitory H_2O_2: a possible counteroffensive strategy for interspecies competition. Mol. Microbiol. **63**, 872–880 CrossRef PubMed

4 Tong, H. C., Chen, W., Shi, W. Y., Qi, F. X. and Dong, X. Z. (2008) SO-LAAO, a novel L-amino acid oxidase that enables *Streptococcus oligofermentans* to outcompete *Streptococcus mutans* by generating H_2O_2 from peptone. J. Bacteriol. **190**, 4716–4721 CrossRef PubMed

5 Boggs, J. M., South, A. H. and Hughes, A. L. (2012) Phylogenetic analysis supports horizontal gene transfer of L-amino acid oxidase gene in *Streptococcus oligofermentans*. Infect. Genet. Evol. **12**, 1005–1009 CrossRef PubMed

6 Wierenga, R. K., Terpstra, P. and Hol, W. G. J. (1986) Prediction of the occurrence of the ADP-binding β-α-β-fold in proteins, using an amino-acid-sequence fingerprint. J. Mol. Biol. **187**, 101–107 CrossRef PubMed

7 Pawelek, P. D., Cheah, J., Coulombe, R., Macheroux, P., Ghisla, S. and Vrielink, A. (2000) The structure of L-amino acid oxidase reveals the substrate trajectory into an enantiomerically conserved active site. EMBO J. **19**, 4204–4215 CrossRef PubMed

8 Geueke, B. and Hummel, W. (2002) A new bacterial L-amino acid oxidase with a broad substrate specificity: purification and characterization. Enzyme Microb. Technol. **31**, 77–87

9 Pollegioni, L., Motta, P. and Molla, G. (2013) L-Amino acid oxidase as biocatalyst: a dream too far? Appl. Microbiol. Biotechnol. **97**, 9323–9341 CrossRef PubMed

10 Du, X. Y. and Clemetson, K. J. (2002) Snake venom L-amino acid oxidases. Toxicon **40**, 659–665 CrossRef PubMed

11 Umhau, S., Pollegioni, L., Molla, G., Diederichs, K., Welte, W., Pilone, M. S. and Ghisla, S. (2000) The X-ray structure of D-amino acid oxidase at very high resolution identifies the chemical mechanism of flavin-dependent substrate dehydrogenation. Proc. Natl. Acad. Sci. U.S.A. **97**, 12463–12468 CrossRef PubMed

12 Pollegioni, L., Piubelli, L., Sacchi, S., Pilone, M. S. and Molla, G. (2007) Physiological functions of D-amino acid oxidases: from yeast to humans. Cell. Mol. Life Sci. **64**, 1373–1394 CrossRef PubMed

13 Pollegioni, L. and Molla, G. (2011) New biotech applications from evolved D-amino acid oxidases. Trends Biotechnol. **29**, 276–283 CrossRef PubMed

14 Zhou, P., Liu, L., Tong, H. and Dong, X. (2012) Role of operon *aao*$_{So}$-*mutT* in antioxidant defense in *Streptococcus oligofermentans*. PLoS ONE **7**, e38133 CrossRef PubMed

15 Lyles, G. A. and Chalmers, J. (1995) Aminoacetone metabolism by semicarbazide-sensitive amine oxidase in rat aorta. Biochem. Pharmacol. **49**, 416–419 CrossRef PubMed

16 Molla, G., Sacchi, S., Bernasconi, M., Pilone, M. S., Fukui, K. and Pollegioni, L. (2006) Characterization of human D-amino acid oxidase. FEBS Lett. **580**, 2358–2364 CrossRef PubMed

17 Volontè, F., Pollegioni, L., Molla, G., Frattini, L., Marinelli, F. and Piubelli, L. (2010) Production of recombinant cholesterol oxidase containing covalently bound FAD in *Escherichia coli*. BMC Biotechnol. **10**, 33 CrossRef PubMed

18 Molla, G., Piubelli, L., Volonte, F. and Pilone, M. S. (2012) Enzymatic detection of D-amino acids. In Unnatural Amino Acids: Methods and Protocols (Pollegioni, L. and Servi, S., eds), pp. 273–289, Humana Press, Totowa CrossRef

19 Green, M. L. and Lewis, J. B. (1968) The oxidation of aminoacetone by a species of *Arthrobacter*. Biochem. J. **106**, 267–270 PubMed

20 Massey, V. and Hemmerich, P. (1978) Photoreduction of flavoproteins and other biological compounds catalyzed by deazaflavins. Biochemistry **17**, 9–17 CrossRef PubMed

21 Harris, C. M., Molla, G., Pilone, M. S. and Pollegioni, L. (1999) Studies on the reaction mechanism of *Rhodotorula gracilis* D-amino-acid oxidase: role of the highly conserved Tyr-223 on substrate binding and catalysis. J. Biol. Chem. **274**, 36233–36240 CrossRef PubMed

22 Job, V., Marcone, G. L., Pilone, M. S. and Pollegioni, L. (2002) Glycine oxidase from *Bacillus subtilis*: characterization of a new flavoprotein. J. Biol. Chem. **277**, 6985–6993 CrossRef PubMed

23 Caldinelli, L., Iametti, S., Barbiroli, A., Bonomi, F., Piubelli, L., Ferranti, P., Picariello, G., Pilone, M. S. and Pollegioni, L. (2004) Unfolding intermediate in the peroxisomal flavoprotein D-amino acid oxidase. J. Biol. Chem. **279**, 28426–28434 CrossRef PubMed

24 Massey, V. A. (1991) simple method for the determination of redox potentials. In In Flavins and Flavoproteins (Curti, B., Ronchi, S. and Zanetti, G., eds), pp. 59–66, Walter de Gruyter & Co., Berlin

25 Pollegioni, L., Porrini, D., Molla, G. and Pilone, M. S. (2000) Redox potentials and their pH dependence of D-amino acid oxidase of *Rhodotorula gracilis* and *Trigonopsis variabilis*. Eur. J. Biochem. **267**, 6624–6632 CrossRef PubMed

26 Kabsch, W. (2010) XDS. Acta Crystallogr. D Biol. Crystallogr. **66**, 125–132 CrossRef PubMed

27 Evans, P. (2006) Scaling and assessment of data quality. Acta Crystallogr. D Biol. Crystallogr. **62**, 72–82 CrossRef PubMed

28 Leslie, A. G. W. (2003) MOSFLM 6.2.3 User Guide, MRC Laboratory of Molecular Biology, Cambridge

29 Storoni, L. C., McCoy, A. J. and Read, R. J. (2004) Likelihood-enhanced fast rotation functions. Acta Crystallogr. D Biol. Crystallogr. **60**, 432–438 CrossRef PubMed

30 Murshudov, G. N., Vagin, A. A. and Dodson, E. J. (1997) Refinement of macromolecular structures by the maximum-likelihood method. Acta Crystallogr. D Biol. Crystallogr. **53**, 240–255 CrossRef PubMed

31 Emsley, P. and Cowtan, K. (2004) Coot: model-building tools for molecular graphics. Acta Crystallogr. D Biol. Crystallogr. **60**, 2126–2132 CrossRef PubMed

32 Chen, V. B., Arendall, W. B., Headd, J. J., Keedy, D. A., Immormino, R. M., Kapral, G. J., Murray, L. W., Richardson, J. S. and Richardson, D. C. (2010) MolProbity: all-atom structure validation for macromolecular crystallography. Acta Crystallogr. D Biol. Crystallogr. **66**, 12–21 CrossRef PubMed

33 Pollegioni, L., Molla, G., Sacchi, S., Rosini, E., Verga, R. and Pilone, M. S. (2008) Properties and applications of microbial D-amino acid oxidases: current state and perspectives. Appl. Microbiol. Biotechnol. **78**, 1–16 CrossRef PubMed

34 Caldinelli, L., Pedotti, M., Motteran, L., Molla, G. and Pollegioni, L. (2009) FAD binding in glycine oxidase from *Bacillus subtilis*. Biochimie **91**, 1499–1508 CrossRef PubMed

35 Hefti, M. H., Vervoort, J. and van Berkel, W. J. (2003) Deflavination and reconstitution of flavoproteins. Eur. J. Biochem. **270**, 4227–4242 CrossRef PubMed

36 Caldinelli, L., Iametti, S., Barbiroli, A., Bonomi, F., Fessas, D., Molla, G., Pilone, M. S. and Pollegioni, L. (2005) Dissecting the structural determinants of the stability of cholesterol oxidase containing covalently bound flavin. J. Biol. Chem. **280**, 22572–22581 CrossRef PubMed

37 Louis-Jeune, C., Andrade-Navarro, M. A. and Perez-Iratxeta, C. (2012) Prediction of protein secondary structure from circular dichroism using theoretically derived spectra. Proteins **80**, 374–381 CrossRef

38 Massey, V. and Hemmerich, P. (1980) Active-site probes of flavoproteins. Biochem. Soc. Trans. **8**, 246–257 PubMed

39 Macheroux, P., Seth, O., Bollschweiler, C., Schwarz, M., Kurfurst, M., Au, L. C. and Ghisla, S. (2001) L-Amino-acid oxidase from the Malayan pit viper *Calloselasma rhodostoma*: comparative sequence analysis and characterization of active and inactive forms of the enzyme. Eur. J. Biochem. **268**, 1679–1686 CrossRef PubMed

40 Sartori, A., Mano, C. M., Mantovani, M. C., Dyszy, F. H., Massari, J., Tokikawa, R., Nascimento, O. R., Nantes, I. L. and Bechara, E. J. (2013) Ferricytochrome (*c*) directly oxidizes aminoacetone to methylglyoxal, a catabolite accumulated in carbonyl stress. PLoS ONE **8**, e57790 CrossRef PubMed

41 Holm, L. and Rosenström, P. (2010) Dali server: conservation mapping in 3D. Nucleic Acids Res. **38**, W545–W549 CrossRef PubMed

42 Dym, O. and Eisenberg, D. (2001) Sequence-structure analysis of FAD-containing proteins. Protein Sci. **10**, 1712–1728 CrossRef PubMed

43 Song, H., Parsons, M. R., Rowsell, S., Leonard, G. and Phillips, S. E. (1999) Crystal structure of intact elongation factor EF-Tu from *Escherichia coli* in GDP conformation at 2.05 Å resolution. J. Mol. Biol. **285**, 1245–1256 CrossRef PubMed

44 Corbett, K. D. and Berger, J. M. (2003) Structure of the topoisomerase VI-B subunit: implications for type II topoisomerase mechanism and evolution. EMBO J. **22**, 151–163 CrossRef PubMed

45 Krissinel, E. and Henrick, K. (2005) Detection of protein assemblies in crystals. Lect. Notes Comput. Sci. **3695**, 163–174 CrossRef

46 Massey, V. and Ganther, H. (1965) On the interpretation of the absorption spectra of flavoproteins with special reference to D-amino acid oxidase. Biochemistry **4**, 1161–1173 CrossRef PubMed

47 Dutra, F., Knudsen, F. S., Curi, D. and Bechara, E. J. H. (2001) Aerobic oxidation of aminoacetone, a threonine catabolite: Iron catalysis and coupled iron release from ferritin. Chem. Res. Toxicol. **14**, 1323–1329 CrossRef PubMed